Magnetic Effects of Nonmagnetic Impurities in Gapped Short-Range Resonating Valence Bond Spin Liquids

Md Zahid Ansari and Kedar Damle
Department of Theoretical Physics, Tata Institiute of Fundamental Research, Mumbai 400 005, India

(Received 1 February 2024; accepted 7 May 2024; published 29 May 2024)

We study the effect of a small density n_v of quenched nonmagnetic impurities, i.e., vacancy disorder, in gapped short-range resonating valence bond (RVB) spin liquid states and valence bond solid (VBS) states of quantum magnets. We argue that a large class of short-range RVB liquids are stable to vacancy disorder at small n_v on the kagome lattice, while the corresponding states on triangular, square, and honeycomb lattices are unstable to vacancy disorder at any nonzero n_v due to the presence of emergent vacancy-induced local moments. In contrast, VBS states are argued to be generically unstable (independent of lattice geometry) to vacancy disorder at any nonzero n_v due to such a local-moment instability. Our arguments rely in part on an analysis of the statistical mechanics of maximally packed dimer covers of the diluted lattice, and are fully supported by our computational results on $O(N)$ symmetric designer Hamiltonians. These arguments also imply that short-range RVB spin liquid states are generically unstable to bond dilution on all these lattices.

DOI: 10.1103/PhysRevLett.132.226504

The original proposal of Anderson [1,2] for a quantum spin liquid state of insulating magnets used a nearest neighbor resonating valence bond (RVB) picture of the many-body ground state. In any term of the corresponding wave function, each spin $S = 1/2$ makes a singlet valence bond with one of its neighbors, and the full quantum state is then a superposition over all possible ways in which this can be done. In more general gapped short-range RVB states, the valence bonds can extend to further neighbors, but are limited in range by a characteristic scale ξ_{RVB} [3].

Although the ground state for the particular case considered originally, namely that of the spin $S = 1/2$ Heisenberg antiferromagnet on the triangular lattice, is now known [4–10] to not be of this RVB liquid type, this proposal sparked many of the developments [11–19] that contributed to our modern understanding of such spin liquid states and their characterization in terms of topological order [20–24]. This theoretical progress has also led to experimental efforts aimed at identifying candidate materials that realize such RVB spin liquid states [25–27].

Part of the difficulty in reaching a definite conclusion about spin liquid behavior in any material is that the simplest phenomenological characterization of a spin liquid is a negative one: A spin liquid displays no magnetic order of any kind, nor do the spins form a definite static pattern of singlet valence bonds that breaks the symmetry of the underlying crystal structure, as is the case in a valence-bond solid (VBS) state. It is thus defined by what is *not seen* in the corresponding experiments.

As a result, the experimental search for spin liquids is challenging even if material imperfections and quenched disorder effects are absent, and their presence only adds to the challenge [26–31]. Short-range RVB spin liquids are expected to be stable to weak bond disorder (exchange disorder) while being destabilized by strong bond disorder, while VBS states are predicted to be unstable even to weak bond disorder [32]. Here, we focus on another important source of disorder, namely non-magnetic substitutional impurities [28–30], which can be modeled theoretically as missing spins or static vacancies, and can serve as a probe of the underlying many-body state [33–42]. We argue that local moments form in the vicinity of each vacancy in VBS states even when the vacancies are isolated, i.e., well separated from each other, while such local moments arise in gapped short-range RVB spin liquids *only* if the maximum matchings (maximally packed dimer covers) of the diluted lattice have a nonzero number of monomers, which is typically not the case when the vacancies are isolated [43–45].

On the randomly site-diluted kagome lattice, we find at low dilution that the largest connected "bulk" component of the lattice hosts at most one such vacancy-induced monomer or local moment; the bulk density of such local moments is thus zero in this regime. In contrast, on randomly site-diluted triangular, square, and honeycomb lattices, certain vacancy clusters that generically occur with nonzero bulk density lead to a bulk density of such monomers (and hence local moments) situated inside well-demarcated "$\mathcal{R}$-type regions" whose geometry has been studied previously [46,47] in other contexts.

We argue that such a bulk density of vacancy-induced emergent local moments represents an instability of the

system since the real ground state is then determined by the many-body wave function of this system of emergent local moments. Thus, we conclude that gapped short-range RVB liquids are stable at small n_v on the kagome lattice, while such states on the triangular, square, and honeycomb lattices have a local moment instability at small n_v. In contrast, VBS states are always unstable at small n_v independent of lattice geometry.

We first explore the contrasting consequences of site dilution on gapped short-range RVB and VBS states by working within the quantum dimer model (QDM) framework of Rokhsar and Kivelson, where each dimer represents a nearest-neighbor singlet [12,13]. Although this framework does not make any explicit reference to further neighbor valence bonds, the effects of matrix elements to such states are encoded via additional terms in the quantum dimer model Hamiltonian [12].

Within this framework, it is clear that the effect of vacancies depends crucially on whether the diluted lattice has perfect matchings (perfect dimer covers). If it does, then it typically has exponentially (in the lattice size) many such perfect matchings due to the possibility of local rearrangements of dimers. If it does not have perfect matchings, then a minimum number of sites have to be left unmatched in any *maximum matching* of the lattice, and the unmatched sites host "monomers" of the maximally packed dimer cover. In such cases, there are typically exponentially many such maximum matchings. Since such an unmatched site is associated with a free spin, these monomers necessarily correspond to emergent vacancy-induced local moments, independent of whether the ground state is an RVB liquid or a VBS state.

Our key point is this: In a gapped short-range RVB liquid state, there is no energetic preference for any particular arrangement of the singlet valence bonds. Therefore, as long as the diluted lattice has exponentially many perfect dimer covers to form a resonating valence bond state, the system is expected to remain in such an RVB state even at nonzero n_v. Thus, vacancies induce the formation of emergent local moments in such RVB states *only if* there are monomers in the maximum matchings of the diluted lattice. In contrast, when the state has VBS order, there is a preferred ordered arrangement of valence bonds. This cannot be maintained on a diluted lattice even if it has perfect matchings: Consider for instance a triangular or square lattice with just two isolated vacancies far apart. Although perfect matchings are possible in this case [43–45], any such singlet state corresponding to a fully-packed arrangement of dimers necessarily leads to a domain wall (in the VBS order parameter) connecting the two vacancy locations [48,49]. The resulting domain wall energy cost (which scales with its length) makes it energetically favourable to eliminate such domain walls by keeping the VBS order intact except in the immediate vicinity of each vacancy. This is achieved by the formation of local moments that are spread out on sites adjacent to each vacancy. Thus, in a VBS ordered system, individual vacancies seed local moments in their vicinity even when they are well separated from each other and perfect dimer covers exist. Clearly, these conclusions apply equally well to RVB and VBS states of bipartite as well as nonbipartite quantum magnets.

Although this argument seems to rely very crucially on the nearest-neighbor nature of singlet valence bonds in the ground state wave function, we nevertheless expect the conclusions to be valid more generally for gapped short-range RVB or VBS states. Indeed, the same conclusions also follow (without relying on any nearest-neighbor singlet wave functions) within a $1/N$ expansion approach [16,50–52] to SU(N) and SO(N) symmetric generalizations [50–59] that have been useful in previous studies of the competition between Neel, VBS, and RVB states of quantum magnets [51–68]. These have a Hamiltonian comprised of nearest-neighbor singlet projectors:

$$H = -\frac{J_m}{N}\sum_{\langle r_1 r_2\rangle}\sum_{\alpha,\beta}|\alpha\rangle_{r_1}|\alpha\rangle_{r_2}\langle\beta|_{r_1}\langle\beta|_{r_2} + \cdots, \quad (1)$$

where $\langle r_1 r_2\rangle$ denotes nearest-neighbor links connecting adjacent sites, the "color" indices α and β denote N possible states of the "spins," and the ellipses denote possible additional multispin interactions acting on all the spins of a single plaquette or groups of adjacent plaquettes of the lattice. On a nonbipartite lattice, H has global O(N) symmetry, with the colors α and β transforming in the fundamental representation of O(N) [51,52]. On a bipartite lattice, r_1 and r_2 always belong to opposite sublattices, and H has enhanced global SU(N) symmetry [16,50], with the colors on A (B) sublattice sites transforming in the fundamental (complex conjugate of the fundamental) representation of SU(N). (In both cases, the additional terms represented by ellipses respect the corresponding symmetry.) Put another way, H always commutes with all the Hermitean antisymmetric generators $\mathcal{A}^{\rm tot}_{\alpha\beta} = \sum_r \mathcal{A}_{\alpha\beta}(r)$ ($\alpha < \beta$) of global O(N) transformations of the colors. Additionally, on bipartite lattices, it also commutes with the symmetric generators $\mathcal{S}^{\rm tot}_{\alpha\beta} = \sum_r (-1)^r \mathcal{S}_{\alpha\beta}(r)$ ($\alpha < \beta$) and the diagonal generators $\mathcal{Q}^{\rm tot}_{\alpha\alpha} = \sum_r (-1)^r \mathcal{Q}_{\alpha\alpha}(r)$ ($\alpha = 1, 2 \ldots N-1$, and no sum over the repeated index implied) that enlarge the global symmetry group to SU(N). Here, $(-1)^r = +1$ [$(-1)^r = -1$] for r belonging to the $A(B)$ sublattice, and

$$\begin{aligned}
\mathcal{A}_{\alpha\beta}(r) &= -i(|\alpha\rangle_r\langle\beta|_r - |\beta\rangle_r\langle\alpha|_r) \quad \forall \text{ pairs } \alpha < \beta,\\
\mathcal{S}_{\alpha\beta}(r) &= (|\alpha\rangle_r\langle\beta|_r + |\beta\rangle_r\langle\alpha|_r) \quad \forall \text{ pairs } \alpha < \beta,\\
\mathcal{Q}_{\alpha\alpha}(r) &= (|\alpha\rangle_r\langle\alpha|_r - 1/N) \quad \forall \ \alpha = 1 \ldots N-1. \qquad (2)
\end{aligned}$$

In the large-N limit without disorder, each perfect dimer cover of the lattice gives a degenerate ground state in both

cases, with the dimers representing SU(N) or O(N) singlets. At leading order in $1/N$, the low-energy physics is then controlled by an effective quantum dimer model Hamiltonian [16,50–52]. Generalizing to the diluted case, we see that the ground state degeneracy at $N = \infty$ now corresponds either to fully-packed dimer covers of the lattice, or to the maximally-packed dimer covers if no perfect matchings exist. In the latter case, the monomers of a maximum matching correspond to free SU(N) or O(N) spins. At leading order in $1/N$, one obtains an effective Hamiltonian that acts within this low-energy subspace. This has the form of a quantum monomer-dimer model in the general case, with ring exchange and monomer hopping terms acting within the ensemble of maximum matchings. At higher orders, additional terms are generated, which act on groups of contiguous bonds and plaquettes. From this structure of the low-energy theory, we see that our previous conclusions regarding vacancy-induced local moments in VBS and RVB states apply to these SU(N) and O(N) generalizations at a finite N so long as the corresponding ground state is accessible perturbatively in $1/N$.

In addition, we see that the perturbatively generated interactions J_{eff} between these emergent local moments only act within each connected component of a diluted lattice. Because of the gapped nature of the parent state, these effective interaction J_{eff} are also expected to be parametrically smaller than the microscopic exchange coupling J_m both in the gapped VBS case, and in the gapped short-range RVB case. Although the form of these interactions is expected to depend sensitively on the microscopic Hamiltonian, the mere fact of their existence implies that a nonzero bulk density of such moments generically signals an instability of the parent state independent of these details [32]. This is because the long-distance structure of the ground state is now controlled by the many-body wave function of this system of emergent local moments. Clearly, such a bulk density of emergent local moments must also give rise to a vacancy-induced contribution $\chi_{\text{imp}} \propto 1/T$ to the thermodynamic susceptibility at low but not too low temperatures in the range $J_{\text{eff}} \ll T \ll J_m$. This serves as a diagnostic for the corresponding local moment instability.

Putting all these arguments together, we are thus led to conclude that short-range VBS states always have a local moment instability at small n_v, while short-range RVB states are unstable only if the dilution leads to a bulk density of monomers in the maximum matchings of the diluted lattice. With this in mind, we turn our attention to the monomers in maximum matchings of randomly site-diluted lattices of interest to us. The results of Ref. [46] and Ref. [47] make it clear that maximum matchings of site-diluted square, honeycomb, and triangular lattices have a nonzero bulk density of monomers. For the kagome case, we supplement this with a computational study using the implementation of Edmonds's maximum matching algorithm given in Ref. [69]. We find that the situation is dramatically different: Each connected component (of the diluted kagome lattice) with an odd number of sites hosts exactly one monomer, while connected components with an even number of sites have a perfect dimer cover, i.e., they host no monomers.

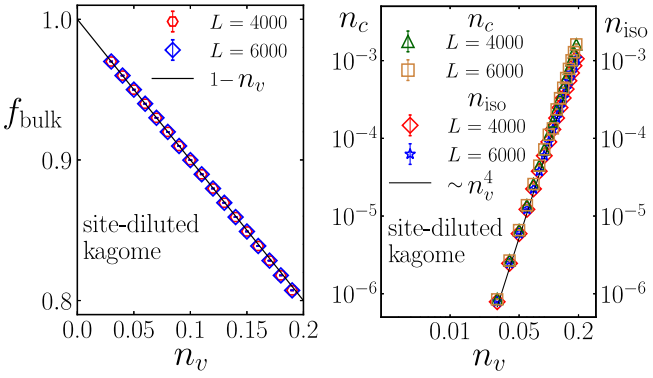

FIG. 1. Left panel: The measured fraction f_{bulk} of sites in the largest connected bulk component of the site-diluted kagome lattice is fit well by $f_{\text{bulk}}(n_v) = 1 - n_v$ in the small-n_v limit. Right panel: In this limit, the number density n_c of connected components of the site-diluted kagome lattice is dominated by the number density n_{iso} of single-site clusters, which scales as $\sim n_v^4$. We have checked that each such connected component of even size (number of sites) is perfectly matched by any maximum matching, while each such odd-sized connected component hosts exactly one monomer, implying that the *bulk* density of monomers is zero.

As a result, as the data in Fig. 1 shows, the bulk density of monomers vanishes for small n_v (i.e., below the geometric percolation threshold of the diluted kagome lattice), since the number of sites in the largest connected component of an $L \times L$ diluted kagome lattice scales as L^2 in the thermodynamic limit, while the mean number of monomers in this component is 0.5. Indeed, we find that essentially all the monomers of any maximum matching of the diluted graph are associated with small disconnected fragments of the diluted lattice at small n_v, with the fraction of monomers corresponding to isolated single-site clusters approaching unity as $n_v \to 0$.

In the kagome spin liquid case, we thus expect vacancy disorder to only lead to at most a single local moment on each individual connected component of the disordered lattice, including on the largest "bulk" component. Being in different fragments of the lattice, these isolated local moments are not expected to interact with each other via the effective couplings J_{eff}. Instead, they represent an essentially decoupled population of free spins that coexist with the bulk spin liquid state.

Therefore, we conclude that gapped short-range RVB spin liquid states are stable at small n_v on the kagome lattice, but have a vacancy-induced local moment instability at any nonzero n_v on square, honeycomb and triangular lattices. For a reliable computational test of our arguments and this

conclusion, we need examples of model Hamiltonians that exhibit such ground states while being amenable to large-scale sign-free quantum Monte Carlo (QMC) studies. When such model systems can be identified, the most direct and straightforward test applicable to both SU(N) and O(N) generalizations would involve studying the effect of vacancies on the susceptibility $\chi^{\mathcal{A}}$ to a uniform field that couples to $\mathcal{A}^{\rm tot}_{\alpha\beta}$ (for any pair $\alpha < \beta$). This would be the analog of the susceptibility to a uniform external field that couples to $S^{\rm tot}_y$ in SU(2) symmetric bipartite systems. However, this susceptibility is not readily measurable in QMC simulations that work in the color (S^z) basis, which are, however, capable of measuring susceptibilities to fields that couple to diagonal operators in the color basis. For SU(N) symmetric designer Hamiltonians on bipartite lattices, this is not a constraint, since one can equivalently measure the susceptibility $\chi^{\mathcal{Q}}$ to a field that couples to $\mathcal{Q}^{\rm tot}_{\alpha\alpha}$ (for any α), since this is equivalent by SU(N) symmetry to $\chi^{\mathcal{A}}$.

Clearly, this is not an option for the O(N) generalizations on nonbipartite lattices. However, this difficulty is not a serious obstacle for the following reason: Such emergent local moments are expected to be essentially free in a broad temperature range $J_{\rm eff} \ll T \ll J_m$. In the bipartite SU($N$) symmetric case, it is therefore clear that they will lead to a Curie tail not just in $\chi^{\mathcal{Q}}$, but also in the susceptibility χ to a field that couples to $n^{\rm tot}_{\alpha\alpha}$ (for any α), where $n^{\rm tot}_{\alpha\alpha}$ differs from $\mathcal{Q}_{\alpha\alpha}$ by the absence of the alternating sign $(-1)^r$ in its definition: $n^{\rm tot}_{\alpha\alpha} = \sum_r \mathcal{Q}_{\alpha\alpha}(r)$ (for $N = 2$, this is the $\hat{z}$ component of the Néel order parameter). Indeed, the difference between χ and $\chi^{\mathcal{Q}}$ will become visible only at $T \sim J_{\rm eff} \ll J_m$. This suggests vacancy-induced local moments will lead to a Curie tail in χ in the nonbipartite case too, and this can serve as an alternate diagnostic test. [For $N > 2$, $n^{\rm tot}_{\alpha\alpha}$ corresponds to the nematic order parameter in such O(N) models].

Examples of designer Hamiltonians with a gapped short-range RVB liquid ground state are in short supply compared to the variety of different models that display VBS ground states [51–68]. Fortunately for our purposes, recent QMC results have established the presence of a gapped short-range RVB liquid ground state for the nearest-neighbor O(N) projector Hamiltonian H [Eq. (1)] with $N > 9$ on the kagome lattice. Therefore, we focus on this O(N) kagome RVB liquid and use large-scale stochastic series expansion (SSE) QMC [70–76] to compute $\chi_{\rm imp}(T) = \chi_{\rm disordered} - \chi_{\rm pure}$, the vacancy-induced change in the static susceptance:

$$\chi = \frac{1}{N-1}\sum_{\alpha=1}^{N-1}\sum_{r,r'}\int_0^\beta \langle \mathcal{Q}_{\alpha\alpha}(r,\tau)\mathcal{Q}_{\alpha\alpha}(r',0)\rangle d\tau, \quad (3)$$

with $\beta = 1/T$ being the inverse temperature. We contrast it with vacancy effects on the same quantity in the triangular lattice O(N) model with nearest-neighbor couplings J_m [Eq. (1)] and additional four-spin interactions of strength Q_2 on four-site plaquettes of the triangular lattice, since this is known to have a VBS ordered ground state for $N > 5$ and large enough values of Q_2/J_m. On both lattices, we consider two disorder configurations, one consisting of two isolated vacancies at distance $L/2$ in an $L \times L$ sample, and the other consisting of two $\mathcal{R}$-type regions at the same distance, each of which traps one monomer of a maximum matching.

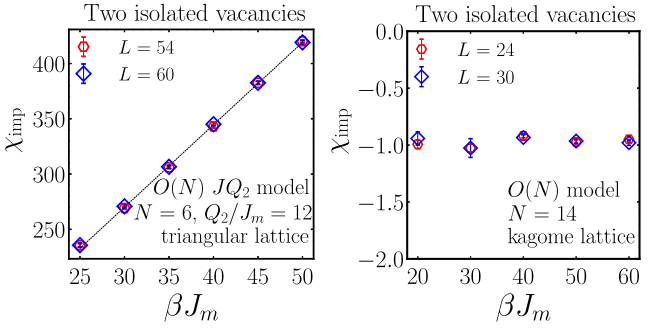

FIG. 2. Left panel: In the triangular lattice O(N) model for values of N in the VBS phase, two isolated vacancies separated by the maximal distance of $L/2$ on an $L \times L$ lattice with L^2 unit cells and periodic boundary conditions give rise to a Curie tail, $\chi_{\rm imp} \propto 1/T \equiv \beta$, in the impurity susceptibility $\chi_{\rm imp}$ defined in the main text. The straight line is a guide to the eye. Right panel: In the kagome case, there is no such Curie tail for values of N in the short-range RVB phase.

In Fig. 2, we show our results for $\chi_{\rm imp}$ corresponding to two isolated vacancies separated by $L/2$ in $L \times L$ triangular and kagome lattice O(N) models for values of N in the VBS and short-range RVB phases, respectively. These results demonstrate that isolated vacancies give rise to a

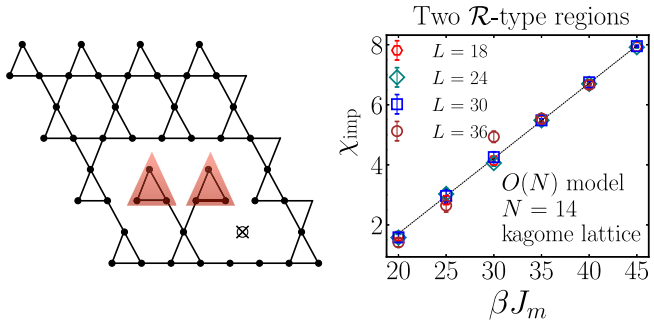

FIG. 3. Left panel: A small $\mathcal{R}$-type region connected to the bulk of the lattice is constructed by deleting a set of bonds in the vicinity of a single vacancy. Any maximum matching of the kagome lattice has a single monomer trapped inside it. Right panel: Impurity susceptibility $\chi_{\rm imp}$ (defined in the text) of the kagome lattice $O(N)$ model due to two such $\mathcal{R}$-type regions separated by $L/2$ in an otherwise pure $L \times L$ kagome lattice with L^2 unit cells and periodic boundary conditions shows clear evidence of a Curie tail $\chi_{\rm imp} \propto 1/T \equiv \beta$ for N in the RVB liquid phase. The straight line is a guide to the eye.

Curie tail in $\chi_{\rm imp}$ in the VBS case but not in the RVB case, confirming one key part of our argument. In Fig. 3, we display a pattern of bond dilution on the kagome lattice that gives rise to an $\mathcal{R}$-type region that traps a single monomer. In addition, we display our data for $\chi_{\rm imp}$ for an $L \times L$ kagome lattice $O(N)$ model with two such $\mathcal{R}$-type regions separated by $L/2$ for a value of N in the RVB liquid phase. Clearly, such monomer-carrying regions give rise to such a Curie tail even in the RVB case, in contrast to isolated vacancies, which do not. This confirms the other key part of our argument. In addition, our results (not shown) confirm that such $\mathcal{R}$-type regions do give rise (exactly as expected) to a Curie tail in $\chi_{\rm imp}$ in the triangular lattice VBS state too. Finally, we note that *bond dilution* (modeling missing exchange pathways) is expected to lead to a nonzero monomer density even on the kagome lattice (as is clear from the example in Fig. 3). Therefore, we conclude that short-range RVB spin liquid states are generically unstable to bond dilution independent of lattice geometry, although they are expected to be stable [32] to weak exchange disorder.

We thank Leon Balents and Subir Sachdev for a useful discussion, Richard Anstee for an informative correspondence about Refs. [43–45] from the mathematical literature, Souvik Kundu and Ritesh Bhola for fruitful collaborations on related work, and departmental system administrators K. Ghadiali and A. Salve for help with cluster related issues. K. D. gratefully acknowledges the hospitality of IISER Pune and stimulating discussions with Deepak Dhar while finalizing the draft of this manuscript. The work of M. Z. A. was supported by a graduate fellowship of the DAE, India at the Tata Institute of Fundamental Research (TIFR). K. D. was supported at the TIFR by DAE, India, and in part by a J. C. Bose Fellowship (JCB/2020/000047) of SERB, DST India, and by the Infosys-Chandrasekharan Random Geometry Center (TIFR). All computations were performed using departmental computational resources of the Department of Theoretical Physics, TIFR, and additional resources supported by a J. C. Bose Fellowship grant (JCB/2020/000047).

[1] P. Anderson, Resonating valence bonds: A new kind of insulator?, Mater. Res. Bull. **8**, 153 (1973).
[2] P. Fazekas and P. W. Anderson, On the ground state properties of the anisotropic triangular antiferromagnet, Philos. Mag. **30**, 423 (1974).
[3] S. Liang, B. Doucot, and P. W. Anderson, Some new variational resonating-valence-bond-type wave functions for the spin-$\frac{1}{2}$ antiferromagnetic Heisenberg model on a square lattice, Phys. Rev. Lett. **61**, 365 (1988).
[4] D. A. Huse and V. Elser, Simple variational wave functions for two-dimensional Heisenberg spin-$\frac{1}{2}$ antiferromagnets, Phys. Rev. Lett. **60**, 2531 (1988).
[5] M. P. Gelfand, R. R. P. Singh, and D. A. Huse, Zero-temperature ordering in two-dimensional frustrated quantum Heisenberg antiferromagnets, Phys. Rev. B **40**, 10801 (1989).
[6] R. R. P. Singh and D. A. Huse, Three-sublattice order in triangular- and kagomé-lattice spin-half antiferromagnets, Phys. Rev. Lett. **68**, 1766 (1992).
[7] B. Bernu, C. Lhuillier, and L. Pierre, Signature of Néel order in exact spectra of quantum antiferromagnets on finite lattices, Phys. Rev. Lett. **69**, 2590 (1992).
[8] A. V. Chubukov, S. Sachdev, and T. Senthil, Large-S expansion for quantum antiferromagnets on a triangular lattice, J. Phys. Condens. Matter **6**, 8891 (1994).
[9] L. Capriotti, A. E. Trumper, and S. Sorella, Long-range Néel order in the triangular Heisenberg model, Phys. Rev. Lett. **82**, 3899 (1999).
[10] S. R. White and A. L. Chernyshev, Neél order in square and triangular lattice Heisenberg models, Phys. Rev. Lett. **99**, 127004 (2007).
[11] S. A. Kivelson, D. S. Rokhsar, and J. P. Sethna, Topology of the resonating valence-bond state: Solitons and high-T_c superconductivity, Phys. Rev. B **35**, 8865 (1987).
[12] D. S. Rokhsar and S. A. Kivelson, Superconductivity and the quantum hard-core dimer gas, Phys. Rev. Lett. **61**, 2376 (1988).
[13] R. Moessner and S. L. Sondhi, Resonating valence bond phase in the triangular lattice quantum dimer model, Phys. Rev. Lett. **86**, 1881 (2001).
[14] V. Kalmeyer and R. B. Laughlin, Equivalence of the resonating-valence-bond and fractional quantum Hall states, Phys. Rev. Lett. **59**, 2095 (1987).
[15] I. Affleck and J. B. Marston, Large-n limit of the Heisenberg-Hubbard model: Implications for high-T_c superconductors, Phys. Rev. B **37**, 3774 (1988).
[16] N. Read and S. Sachdev, Some features of the phase diagram of the square lattice SU(N) antiferromagnet, Nucl. Phys. **B316**, 609 (1989).
[17] N. Read and S. Sachdev, Large-N expansion for frustrated quantum antiferromagnets, Phys. Rev. Lett. **66**, 1773 (1991).
[18] S. Sachdev, Kagome and triangular-lattice Heisenberg antiferromagnets: Ordering from quantum fluctuations and quantum-disordered ground states with unconfined bosonic spinons, Phys. Rev. B **45**, 12377 (1992).
[19] G. Misguich, C. Lhuillier, B. Bernu, and C. Waldtmann, Spin-liquid phase of the multiple-spin exchange Hamiltonian on the triangular lattice, Phys. Rev. B **60**, 1064 (1999).
[20] X. G. Wen, Mean-field theory of spin-liquid states with finite energy gap and topological orders, Phys. Rev. B **44**, 2664 (1991).
[21] X. Wen, *Quantum Field Theory of Many-Body Systems: From the Origin of Sound to an Origin of Light and Electrons* (Oxford University Press, New York, 2007).
[22] X. Wen, Colloquium: Zoo of quantum-topological phases of matter, Rev. Mod. Phys. **89**, 041004 (2017).
[23] R. Moessner and J. E. Moore, *Topological Phases of Matter* (Cambridge University Press, Cambridge, England, 2021).
[24] S. Sachdev, *Quantum Phases of Matter* (Cambridge University Press, Cambridge, England, 2023).

[25] M. R. Norman, Colloquium: Herbertsmithite and the search for the quantum spin liquid, Rev. Mod. Phys. **88**, 041002 (2016).

[26] C. Broholm, R. J. Cava, S. A. Kivelson, D. G. Nocera, M. R. Norman, and T. Senthil, Quantum spin liquids, Science **367**, eaay0668 (2020).

[27] L. Clark and A. H. Abdeldaim, Quantum spin liquids from a materials perspective, Annu. Rev. Mater. Res. **51**, 495 (2021).

[28] S.-H. Lee, H. Kikuchi, Y. Qiu, B. Lake, Q. Huang, K. Habicht, and K. Kiefer, Quantum-spin-liquid states in the two-dimensional kagome antiferromagnets $Zn_xCu_{4-x}(OD)_6Cl_2$, Nat. Mater. **6**, 853 (2007).

[29] M. A. de Vries, K. V. Kamenev, W. A. Kockelmann, J. Sanchez-Benitez, and A. Harrison, Magnetic ground state of an experimental $S = 1/2$ kagome antiferromagnet, Phys. Rev. Lett. **100**, 157205 (2008).

[30] E. Häußler, J. Sichelschmidt, M. Baenitz, E. C. Andrade, M. Vojta, and T. Doert, Diluting a triangular-lattice spin liquid: Synthesis and characterization of $NaYb_{1-x}Lu_xS_2$ single crystals, Phys. Rev. Mater. **6**, 046201 (2022).

[31] J. A. M. Paddison, M. Daum, Z. Dun, G. Ehlers, Y. Liu, M. B. Stone, H. Zhou, and M. Mourigal, Continuous excitations of the triangular-lattice quantum spin liquid $YbMgGaO_4$, Nat. Phys. **13**, 117 (2017).

[32] I. Kimchi, A. Nahum, and T. Senthil, Valence bonds in random quantum magnets: Theory and application to $YbMgGaO_4$, Phys. Rev. X **8**, 031028 (2018).

[33] A. W. Sandvik, E. Dagotto, and D. J. Scalapino, Nonmagnetic impurities in spin-gapped and gapless Heisenberg antiferromagnets, Phys. Rev. B **56**, 11701 (1997).

[34] S. Sachdev, C. Buragohain, and M. Vojta, Quantum impurity in a nearly critical two-dimensional antiferromagnet, Science **286**, 2479 (1999).

[35] K. Gregor and O. I. Motrunich, Nonmagnetic impurities in a $S = \frac{1}{2}$ frustrated triangular antiferromagnet: Broadening of ^{13}C NMR lines in $\kappa - (ET)_2Cu_2(CN)_3$, Phys. Rev. B **79**, 024421 (2009).

[36] L. Wang and A. W. Sandvik, Low-energy excitations of two-dimensional diluted Heisenberg quantum antiferromagnets, Phys. Rev. B **81**, 054417 (2010).

[37] S. Ghosh, H. J. Changlani, and C. L. Henley, Schwinger boson mean field perspective on emergent spins in diluted Heisenberg antiferromagnets, Phys. Rev. B **92**, 064401 (2015).

[38] K. H. Höglund, A. W. Sandvik, and S. Sachdev, Impurity induced spin texture in quantum critical 2D antiferromagnets, Phys. Rev. Lett. **98**, 087203 (2007).

[39] R. K. Kaul, R. G. Melko, M. A. Metlitski, and S. Sachdev, Imaging bond order near nonmagnetic impurities in square-lattice antiferromagnets, Phys. Rev. Lett. **101**, 187206 (2008).

[40] A. Banerjee, K. Damle, and F. Alet, Impurity spin texture at a deconfined quantum critical point, Phys. Rev. B **82**, 155139 (2010).

[41] S. Sanyal, A. Banerjee, and K. Damle, Vacancy-induced spin texture in a one-dimensional $S = \frac{1}{2}$ Heisenberg antiferromagnet, Phys. Rev. B **84**, 235129 (2011).

[42] A. Banerjee, K. Damle, and F. Alet, Impurity spin texture at the critical point between Néel-ordered and valence-bond-solid states in two-dimensional SU(3) quantum antiferromagnets, Phys. Rev. B **83**, 235111 (2011).

[43] R. Aldred, R. Anstee, and S. Locke, Perfect matchings after vertex deletions, Discrete Math. **307**, 3048 (2007).

[44] R. P. Anstee, J. Blackman, and H. Yang, Perfect matchings in grid graphs after vertex deletions, SIAM J. Discrete Math. **25**, 1754 (2011).

[45] R. P. Anstee, J. Blackman, and H. Yang, Perfect matching after vertex deletions on the grid graph and triangular graph (unpublished).

[46] R. Bhola, S. Biswas, M. M. Islam, and K. Damle, Dulmage-Mendelsohn percolation: Geometry of maximally packed dimer models and topologically protected zero modes on site-diluted bipartite lattices, Phys. Rev. X **12**, 021058 (2022).

[47] R. Bhola and K. Damle, Gallai-Edmonds percolation of topologically protected collective Majorana excitations, arXiv:2311.05634.

[48] M. Levin and T. Senthil, Deconfined quantum criticality and Néel order via dimer disorder, Phys. Rev. B **70**, 220403(R) (2004).

[49] T. Senthil, L. Balents, S. Sachdev, A. Vishwanath, and M. P. A. Fisher, Deconfined criticality critically defined, J. Phys. Soc. Jpn. **74**, 1 (2005).

[50] I. Affleck, Large-n limit of SU(n) quantum "spin" chains, Phys. Rev. Lett. **54**, 966 (1985).

[51] R. K. Kaul, Spin nematics, valence-bond solids, and spin liquids in SO(N) quantum spin models on the triangular lattice, Phys. Rev. Lett. **115**, 157202 (2015).

[52] M. S. Block, J. D'Emidio, and R. K. Kaul, Kagome model for a $\mathbb{Z}_2$ quantum spin liquid, Phys. Rev. B **101**, 020402(R) (2020).

[53] K. Harada, N. Kawashima, and M. Troyer, Néel and spin-Peierls ground states of two-dimensional SU(N) quantum antiferromagnets, Phys. Rev. Lett. **90**, 117203 (2003).

[54] N. Kawashima and Y. Tanabe, Ground states of the SU(N) Heisenberg model, Phys. Rev. Lett. **98**, 057202 (2007).

[55] K. S. D. Beach, F. Alet, M. Mambrini, and S. Capponi, SU(N) Heisenberg model on the square lattice: A continuous-N quantum Monte Carlo study, Phys. Rev. B **80**, 184401 (2009).

[56] J. Lou, A. W. Sandvik, and N. Kawashima, Antiferromagnetic to valence-bond-solid transitions in two-dimensional SU(N) Heisenberg models with multispin interactions, Phys. Rev. B **80**, 180414(R) (2009).

[57] R. K. Kaul and A. W. Sandvik, Lattice model for the SU(N) Néel to valence-bond solid quantum phase transition at large N, Phys. Rev. Lett. **108**, 137201 (2012).

[58] M. S. Block, R. G. Melko, and R. K. Kaul, Fate of $\mathbb{CP}^{N-1}$ fixed points with q monopoles, Phys. Rev. Lett. **111**, 137202 (2013).

[59] S. Kundu, N. Desai, and K. Damle, Competition between Neel, Haldane nematic, plaquette valence bond solid, and (π, π) valence bond solid phases in SU(N) analogs of $S = 1$ square-lattice antiferromagnets, arXiv:2309.12262.

[60] A. W. Sandvik, Evidence for deconfined quantum criticality in a two-dimensional Heisenberg model with four-spin interactions, Phys. Rev. Lett. **98**, 227202 (2007).

[61] R. G. Melko and R. K. Kaul, Scaling in the fan of an unconventional quantum critical point, Phys. Rev. Lett. **100**, 017203 (2008).

[62] A. W. Sandvik, Continuous quantum phase transition between an antiferromagnet and a valence-bond solid in two dimensions: Evidence for logarithmic corrections to scaling, Phys. Rev. Lett. **104**, 177201 (2010).
[63] A. Sen and A. W. Sandvik, Example of a first-order Néel to valence-bond-solid transition in two dimensions, Phys. Rev. B **82**, 174428 (2010).
[64] A. Banerjee, K. Damle, and A. Paramekanti, Néel to staggered dimer order transition in a generalized honeycomb lattice Heisenberg model, Phys. Rev. B **83**, 134419 (2011).
[65] S. Pujari, K. Damle, and F. Alet, Néel-state to valence-bond-solid transition on the honeycomb lattice: Evidence for deconfined criticality, Phys. Rev. Lett. **111**, 087203 (2013).
[66] S. Pujari, F. Alet, and K. Damle, Transitions to valence-bond solid order in a honeycomb lattice antiferromagnet, Phys. Rev. B **91**, 104411 (2015).
[67] A. Iaizzi, K. Damle, and A. W. Sandvik, Field-driven quantum phase transitions in $S = \frac{1}{2}$ spin chains, Phys. Rev. B **95**, 174436 (2017).
[68] A. Iaizzi, K. Damle, and A. W. Sandvik, Metamagnetism and zero-scale-factor universality in the two-dimensional $J - Q$ model, Phys. Rev. B **98**, 064405 (2018).
[69] J. D. Kececioglu and J. Pecqueur, Computing maximum-cardinality matchings in sparse general graphs, in *Proceedings of WAE'98 2nd Workshop on Algorithm Engineering* (Max-Planck-Institut fur Informatik, Saarbrucken, 1998), pp. 121–132.
[70] A. W. Sandvik, A generalization of Handscomb's quantum Monte Carlo scheme-application to the 1D Hubbard model, J. Phys. A **25**, 3667 (1992).
[71] A. W. Sandvik, Stochastic series expansion method with operator-loop update, Phys. Rev. B **59**, R14157 (1999).
[72] O. F. Syljuåsen and A. W. Sandvik, Quantum Monte Carlo with directed loops, Phys. Rev. E **66**, 046701 (2002).
[73] A. W. Sandvik, Computational studies of quantum spin systems, AIP Conf. Proc. **1297**, 135 (2010).
[74] A. W. Sandvik and H. G. Evertz, Loop updates for variational and projector quantum Monte Carlo simulations in the valence-bond basis, Phys. Rev. B **82**, 024407 (2010).
[75] A. Banerjee and K. Damle, Generalization of the singlet sector valence-bond loop algorithm to antiferromagnetic ground states with total spin $S_{\mathrm{tot}} = 1/2$, J. Stat. Mech. (2010) P08017.
[76] N. Desai and S. Pujari, Resummation-based quantum Monte Carlo for quantum paramagnetic phases, Phys. Rev. B **104**, L060406 (2021).